Broadband second harmonic generation by birefringent phase matching in an X-cut $LiNbO_3$ membrane

Aiman Zinaoui[1,*], *Lucas* Grosjean[1], *Martin* Khouri[1], *Antoine* Coste[1], *Miguel Angel* Suarez[1], *Samuel* Queste[1], *Ludovic* Gauthier-Manuel[1], *Laurent* Robert[1], *Mathieu* Chauvet[1], *Nadege* Courjal[1]

[1] FEMTO-ST, Besançon, France

Abstract. We designed an X-cut lithium niobate ($LiNbO_3$) membrane dedicated to type I second harmonic generation (SHG) at telecom wavelength. A competitive conversion efficiency compared to a quasi-phase-matched configuration with the advantage of a broadband response of 100nm is shown.

INTRODUCTION

Frequency conversion is an essential process for any application requiring non-linear functions such as quantum information processing [1], or integrated ultrafast light sources [2].

The most common approach for frequency conversion is based on the use of crystals with a strong second order nonlinear effect such as $LiNbO_3$ and inversing periodically its polarity (PPLN - Periodically Poled Lithium Niobate). By combining this technique with the small footprint of the waveguide, high conversion efficiencies of 33000%/W/cm² have been achieved [3]. However, this conversion is severely limited by a spectral bandwidth typically of few nanometres. A wide band of 100nm has been demonstrated in chirped PPLN platform, at the expense of the conversion efficiency which was reduced to 9.6%/W/cm² [4].

In this context, we propose a frequency doubling/twin photon generator device based on highly confined $LiNbO_3$ waveguide and on modal phase matching. The pump and the SHG signal have a perpendicular polarization which facilitates their separation. But the main interest of the proposed configuration comes from its very wide spectral response of 100nm in the telecom band together with a normalized efficiency approaching 60%/W/cm².

These performances are achieved for a core $LiNbO_3$ waveguide height close to 2µm, a dimension not achievable with the ion slicing fabrication process [5] limited to sub-micron thicknesses. We thus propose a new structuring method allowing a micrometric thickness in a channel waveguide with low insertion losses of 2.8dB [6].

1 PRESENTATION OF THE STRUCTURE

The structure is schematized in Figure 1.a.: it consists of a ridge waveguide suspended on a 500nm $LiNbO_3$ membrane. The dimension of the ridge is directly related to the dispersion of the ordinary and extraordinary effective index of the waveguide thus to the phase-matching condition. In an X-cut configuration, the pump is polarized to excite the TM00 mode, and the SHG is generated on the TE00 orthogonal polarization. This nonlinear region is extended by two adiabatic transitions to the low gradient index waveguides realized by titanium diffusion, which allows insertion losses below 2.8dB with standard SMF28 fibers [6] and selects only the fundamental mode in the nonlinear region.

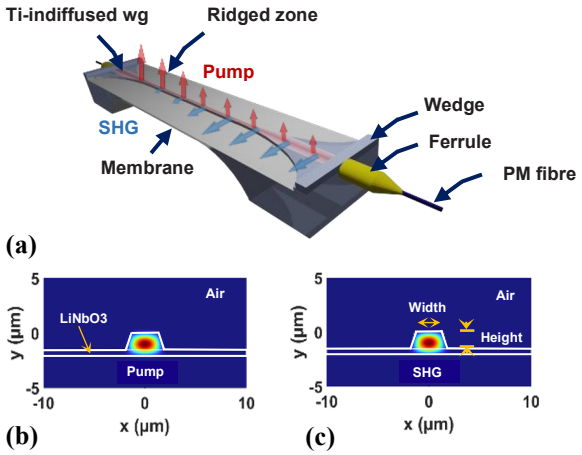

Fig. 1. (a) Schema of the suspended ridge waveguide. The non-linear zone is 1 mm long. (b) COMSOL® simulation of the TM00 mode corresponds to a pump at 1.55µm and neff = 2.17808. (c) TE00 mode simulation corresponds to the SHG at 0.775µm and neff = 2.17805. Both simulations were done for an anisotropic waveguide of height equal to 1.55µm and width of 2.77µm at a fixed temperature equal to 20°C.

The manufacturing process begins with the depositing of a 6 µm wide titanium ribbon waveguide diffused at 1050° for 10 hours. The ridge waveguide is etched on both sides of the diffused titanium waveguide by reactive ion etching (RIE). The membrane is finally inscribed in the material at the back side of the waveguide by dicing-polishing with a precision circular saw (3350 DISCO DAD). The thickness variation between the non-linear phase matching zone and the ends is done adiabatically, using the saw blade footprint: the adiabatic transitions and the membrane is thus realized simultaneously. This fabrication process allows, in comparison with LNOI processes, to save several fabrication steps (bonding, ion implantation, annealing, HF etching), and therefore to ensure a lower energy consumption of fabrication (energy gain estimated of 410kWh for a 4-inch wafer with 150 membranes) while preserving the state of the art insertion losses.

To numerically determine the phase matching conditions, we set the ridge taper angle to 15°, a value

* Corresponding author: aiman.zinaoui@femto-st.fr

derived from experimental results of RIE etching at the MIMENTO clean room. And we determine by finite element method (f.e.m.) with the COMSOL® software the dimensions (height, width) for which the phase matching condition is accomplished.

2 NUMERICAL SIMULATIONS

For the numerical simulation, we consider only the ridge area where the generation of the second harmonic takes place. It is most efficient if the difference between the effective index of the pump and the SHG modes is less than ($\approx 10^{-4}$), which corresponds to an accuracy on the height or width less than ≈10nm. It constitutes a challenging technology to accomplish. As an alternative to geometry control, by exploiting the thermal dispersion of the extraordinary refractive index, we can compensate the phase matching condition as presented in Figure 3.b. Hence, we show that a variation of 120°C is comparable to a variation of 350nm in ridge height, which allows us to release the fabrication constraints while still achieving the phase-matching condition.

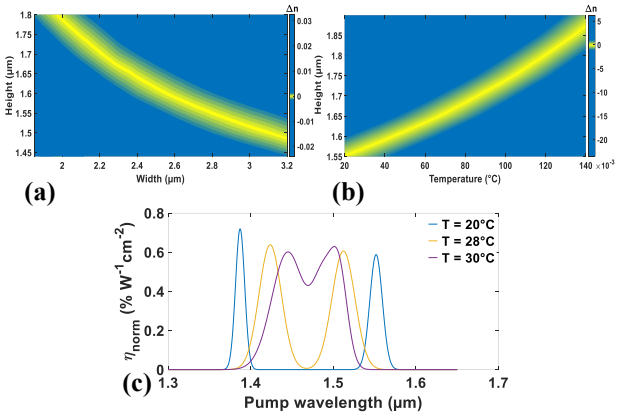

Fig. 3. Phase matching condition ($\Delta n = neff_{SHG} - neff_{Pump}$) as a function of geometry parameter (a) and temperature (b). (a) Variation of ridge height versus width for a pump wavelength equal to 1.55µm and a fixed temperature of 20°C. (b) Variation of ridge height versus temperature at a fixed waveguide width of 2µm. (c) The normalized conversion efficiency as a function of pump wavelength for different temperatures at a fixed height=1.55µm and width=2.77µm for 1mm propagation length

Figure 3.a. shows several possibilities for the size of the ridge. Based on two criteria: technological feasibility and conversion efficiency, we set the ridge parameters at a width of w = 2.77µm and a height of h=1.55µm. The normalized conversion coefficient is given by the following expression [7]:

$$\eta_{norm} = \frac{I_{SHG}}{I_{pump}^2 L^2} = \frac{8\pi^2}{\varepsilon_o c n_{pump}^2 n_{SHG} \lambda_{pump}^2} \frac{\xi^2 d_{eff}^2}{A_{eff}} \qquad (1)$$

Where I_{SHG} and I_{Pump} is the respective SHG and pump intensity, c is the speed of light in vacuum, ε_o is the dielectric permittivity of vacuum, d_{eff} is the nonlinear effective coefficient of order 2 equal to 4.3pm/V, A_{eff} is the effective mode area and ξ is the spatial overlap integral of the two modes of effective index n_{Pump} and n_{SHG}.

We obtain a spatial overlap integral equal to ≈ 99%, an effective mode area of 3.65µm², and a normalized conversion coefficient equal to η_{norm} = 59%/W/cm². These results are obtained at telecom wavelength in an X-cut structure. As shown in Figure 3.c., the temperature is a key parameter to set the SHG phase matching, it allows to tune the central wavelength and passes from a spectral band of 50nm to a wide spectral band of 100nm by increasing the temperature of the sample of about ten degrees.

CONCLUSION

We have theoretically demonstrated the process of type I second harmonic generation in the C-band of optical telecommunications using a technologically accessible structure composed of a ridge waveguide suspended on a 500nm membrane with low energy manufacturing cost. A normalized conversion coefficient equal to 59%/W/cm² at telecom wavelength has been numerically predicted together with a wide band response as large as 100nm.

Reference

1. G. Moody et al (2022) J. Phys. Photonics 4 012501
2. Q. Guo, R. Sekine, L. Ledezma et al. Nat. Photon. 16, 625–631 (2022)
3. T. Park, et al. Optics Letters 47.11 (2022): 2706-2709
4. Xiao Wu, Li Zhang, Zhenzhong Hao, Ru Zhang, Rui Ma, Fang Bo, Guoquan Zhang, and Jingjun Xu, Opt. Lett. 47, 1574-1577 (2022)
5. Y. Jia et al. Appl. Phys. Rev. 8, 011307 (2021)
6. M. Mwangi, F. Behague, A.Coste, J.Safioui, M. Suarez, J. Byiringiro, P. Lutz, C. Clévy, N. Courjal. (2022) Optics Continuum .1
7. C. Wang, H. Zhong, M. Ning, B. Fang, L. Li, Y. Cheng Photonics (2023) 10, 80